Silver Nanoparticle–Reactive Oxygen Species Interactions: Application of a Charging–Discharging Model

ARTICLE *in* THE JOURNAL OF PHYSICAL CHEMISTRY C · MARCH 2011

Impact Factor: 4.77 · DOI: 10.1021/jp111275a

5 AUTHORS, INCLUDING:

Di He
University of New South Wales
19 PUBLICATIONS **316** CITATIONS
SEE PROFILE

Shikha Garg
University of New South Wales
17 PUBLICATIONS **309** CITATIONS
SEE PROFILE

An Ninh Pham
University of New South Wales
23 PUBLICATIONS **438** CITATIONS
SEE PROFILE

T. David Waite
University of New South Wales
316 PUBLICATIONS **9,817** CITATIONS
SEE PROFILE

THE JOURNAL OF PHYSICAL CHEMISTRY C

ARTICLE

pubs.acs.org/JPCC

Silver Nanoparticle−Reactive Oxygen Species Interactions: Application of a Charging−Discharging Model

Di He, Adele M. Jones, Shikha Garg, A. Ninh Pham, and T. David Waite*

School of Civil and Environmental Engineering, University of New South Wales, Sydney, NSW, Australia 2052

Supporting Information

ABSTRACT: The silver-nanoparticle-catalyzed decomposition of hydrogen peroxide (H_2O_2) in pH 9.5 bicarbonate buffer is investigated here with attention given to (i) the mechanism of decomposition, (ii) the role of superoxide in mediating silver nanoparticle re-formation, and (iii) the effect of nanoparticle size on decomposition rate. Silver nanoparticles (AgNPs) of average size between 25.0 and 69.4 nm were synthesized via the reduction of Ag^+ [the dominant Ag(I) species present] by photochemically produced superoxide at pH 9.5 and characterized by UV−visible spectroscopy and dynamic light scattering. The ability of these particles to catalytically decompose H_2O_2 was examined by measuring the decay of H_2O_2 and the approach to steady state in AgNP and Ag^+ concentrations. Additionally, the generation of superoxide on reaction of AgNPs with H_2O_2 was monitored using a chemiluminescence-based method. The second-order rate constants for reaction between AgNPs and H_2O_2 correlated linearly with their average particle size ranging from 35.0 to 3.0 × 10^2 M^{-1} s^{-1} for average sizes between 69.4 and 25.0 nm. A sensitive trap-and-trigger chemiluminescence-based method for hydroxyl radical detection showed no evidence for the presence of hydroxyl radicals, though an inhibitory effect of *tert*-butyl alcohol suggested the presence of a strongly oxidizing species. A process involving the superoxide-mediated charging of silver nanoparticles with subsequent discharge by reaction with oxygen and Ag^+ leading to regeneration of Ag^0 and superoxide is proposed to account for the results obtained.

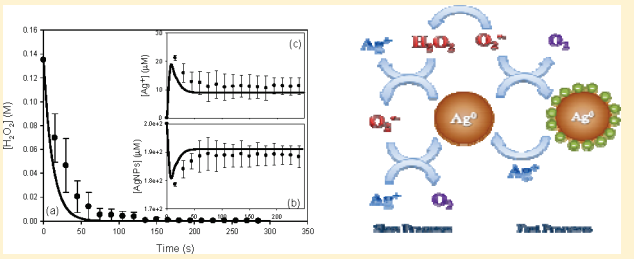

INTRODUCTION

Silver nanoparticles (AgNPs) are one of the most commonly used nanomaterials because of their strong antimicrobial activity.[1−3] However, the mode of antimicrobial action by AgNPs has not as yet been fully elucidated. Possible mechanisms by which AgNPs inhibit microbial growth include: (1) uptake of soluble Ag(I) species followed by disruption of ATP production and DNA replication; (2) direct damage to cell membranes by AgNPs, and (3) AgNP- and Ag^+-mediated generation of reactive oxygen species (ROS), potentially including superoxide ($O_2^{\bullet-}$), hydroxyl radicals ($^{\bullet}OH$), hydrogen peroxide (H_2O_2), and singlet oxygen ($^1O_2$).[3−6]

Application of techniques such as electron spin resonance spectroscopy[7] and fluorescent ROS probes[8,9] provides strong evidence for the generation of ROS by AgNPs (and other silver species). Additionally, Liu and Hurt[10] monitored the generation of H_2O_2 over a time scale of hours to days following the addition of AgNPs to air-saturated aqueous solutions and concluded that $O_2^{\bullet-}$, a precursor of H_2O_2, is formed via the oxidation of AgNPs by oxygen.

In addition to these observations of ROS generation by AgNPs or soluble Ag(I) species, there is compelling evidence that these species are responsible for the strong bactericidal activity of AgNPs and/or Ag(I) species. Mendis et al.[11] indicated that the generation of ROS by AgNPs can lead to a breakdown of membrane and mitochondrial function or cause DNA damage to bacteria. In addition, the loss of bactericidal activity has been observed in the presence of hydroxyl radical, singlet oxygen, and superoxide scavengers.[12−14] The loss of bactericidal activity has also been observed in the presence of catalase, an enzyme that catalyzes the decomposition of hydrogen peroxide into water and oxygen.[13,14]

Although ROS generation by AgNPs is now evident and a relationship between ROS and bactericidal activity of AgNPs is apparent,[15] very little quantification of the reactions between AgNPs and ROS has been reported, including the interaction of AgNPs with H_2O_2, the most stable ROS. As noted above, H_2O_2 has been observed to be produced when AgNPs react with oxygen,[10] most likely via the production of superoxide, $O_2^{\bullet-}$, which readily disproportionates to H_2O_2 in a pH-dependent manner:[16]

$$O_2^{\bullet-} + O_2^{\bullet-} + 2H^+ \rightarrow H_2O_2 + O_2 \qquad (1)$$

Conversely, it is also recognized that AgNPs can catalyze the decomposition of H_2O_2, resulting in the production of superoxide,[17,18] and, through recent investigations in our own laboratory,[19] that superoxide can mediate the reduction of Ag^+ to AgNPs. It therefore appears that a complex interplay among AgNPs, Ag^+, superoxide, and H_2O_2 exists with an understanding

Received: November 27, 2010
Revised: February 5, 2011
Published: March 04, 2011

of these interactions potentially at the core of the bactericidal behavior of silver species. As such, this work is focused on obtaining a better understanding and, to the extent possible, quantification of the interaction between AgNPs and the reactive oxygen species H_2O_2 and $O_2^{\bullet-}$.

An innovative method of producing AgNPs is used in this study involving the reduction of Ag^+ [the major Ag(I) species present] in alkaline solutions using superoxide which, at this pH, disproportionates relatively slowly and is therefore available for reaction with Ag^+.[16] Additionally, at this alkaline pH, the AgNP particles produced do not aggregate, presumably because of high surface charge.[20] As such, the presence of highly charged stabilizers such as borohydride, citrate, or polyvinylpyrrolidone (which may cause complications in studies of interactions of AgNPs with H_2O_2) are not required in order to maintain the synthesized AgNPs in suspension.[21]

EXPERIMENTAL METHODS

Reagents. All chemicals used in this work were analytical reagent grade and were purchased from Sigma unless otherwise stated. All solutions were prepared in ultrapure 18.2 MΩ cm Milli-Q water (Millipore).

All experiments were performed in a 2.0 mM bicarbonate buffer with final pH adjusted to 9.5. This solution was prepared on a daily basis. A 50 mM stock solution of Ag^+ (Ajax Chemicals) was prepared on a weekly basis by dissolving an appropriate amount of $AgNO_3$ in Milli-Q water. A solution containing 4% v/v ethanol, 0.4% v/v acetone (Ajax Chemicals), and 2 mM bicarbonate buffer adjusted to pH 9.5 was prepared for the subsequent photochemical production of $O_2^{\bullet-}$. A 7.5 mM stock solution of diethylenetriaminepentaacetic acid (DTPA) was prepared in Milli-Q water and the ethanol/acetone solution made up to 1 μM DTPA in order to prevent the catalyzed disproportionation of $O_2^{\bullet-}$ by trace metal contaminants. Stock solutions of 10 mM and 1 M H_2O_2 were prepared weekly by dilution of a 30% w/v H_2O_2 solution and standardized by UV−vis spectrometry.[22] Stock solutions of 100 μM Amplex Red (AR; Invitrogen) mixed with 50 U mL^{-1} horseradish peroxidase (HRP; Sigma) for H_2O_2 determination were prepared and stored as described previously.[23] Methyl *Cypridina* luciferin analogue (MCLA, Fluka) reagent, for use in the chemiluminescence (CL) measurement of superoxide, was prepared as 1 μM MCLA in 0.05 M acetate buffer at pH 6.0, stored in a dark glass bottle, and refrigerated at 4 °C when not in use. Phthalhydrazide (Phth, 99%, Aldrich) solutions (for hydroxyl radical detection) were prepared by stirring at 45 °C for several hours until solid was no longer visible. Diperiodatocuprate(III) (DPC) was synthesized following a previously published method.[24] Analytical reagent grade *tert*-butyl alcohol (TBA) (Ajax Chemicals) was employed as hydroxyl radical scavenger. Concentrated nitric acid and sodium hydroxide were used for the adjustment of pH. Experiments were performed at a controlled room temperature of 22 °C.

Production of Silver Nanoparticle Suspensions. AgNPs were produced by the reduction of Ag^+ by photochemically generated $O_2^{\bullet-}$ in a manner identical to that described previously[19] and involved addition of an aliquot of the 50 mM Ag^+ stock solution to the pH 9.5 acetone/ethanol solution prior to UV illumination. The solution was subsequently illuminated [using a Pen-Ray Hg lamp, model 90-0012-01 (11SC-1); primary energy at 254 nm] until the AgNP absorbance at 415 nm reached a maximum value (typically taking approximately 30 s).[19] AgNP suspensions were produced for initial Ag^+ concentrations of 30, 60, 100, and 200 μM with the AgNPs produced in each case characterized as described below. Aliquots of each AgNP suspension were subsequently used in the studies of AgNP-mediated H_2O_2 degradation.

Characterization of the Silver Nanoparticles. AgNPs are able to absorb visible light of a particular wavelength due to the excitation of free surface electrons known as plasmons.[25−28] Hence visible spectrophotometry can be employed to characterize the AgNPs produced in this study. A Cary 50 UV−vis spectrometer (Varian Inc.) was employed to perform scans over 250−550 nm. For roughly spherical AgNPs, surface plasmon resonance (SPR) occurs at approximately 400−450 nm.[29] As noted by Jones et al.,[19] the absorbance associated with SPR for the particles produced by the method described here is similar to that of particles prepared by the direct reduction of Ag^+ by either borohydride or superoxide derived from KO_2. Previous high-resolution transmission electron microscopy of AgNP particles produced in an identical manner to that described here confirmed that the *d*-spacings of the resulting particles were characteristic of zerovalent silver.[19]

Dynamic light scattering (DLS) (Malvern Zetasizer Nano S) with a 633 nm laser source and detection angle of 173° was used to monitor cluster size. A digital correlator was used to develop an autocorrelation function, which was analyzed using the method of cumulants,[29,30] resulting in a *z*-averaged diameter, d_z (intensity-weighted mean hydrodynamic diameter). Knowing the refractive index of the sample, it was also possible to use Mie theory to convert the intensity distribution to a volume distribution. The same instrument was also used to measure electrophoretic mobility of AgNPs with the values obtained subsequently transformed to ζ-potentials using Smoluchowski's approximation.

H_2O_2 Decomposition by Silver Nanoparticles. The interaction between AgNPs and H_2O_2 was followed by measuring the concentrations of H_2O_2, Ag^+, and AgNPs over time following the addition of H_2O_2 to pH 9.5 suspensions of AgNPs.

Low (micromolar) concentrations of H_2O_2 were measured using the Amplex Red (AR) method.[31,32] Samples for H_2O_2 determination were manually withdrawn from the reactor and then mixed in a quartz cuvette with AR/HRP stock solution at final AR and HRP concentrations of 2.0 μM and 1 kU L^{-1}, respectively. The fluorescence of the sample was measured in a Cary Eclipse spectrophotometer using settings described previously.[23] For H_2O_2 quantification, a calibration curve encompassing H_2O_2 concentrations over the range from 75 to 600 nM was obtained.

The degradation of high (millimolar) concentrations of H_2O_2 by AgNPs was monitored spectrophotometrically at 250 nm, where H_2O_2 possesses a molar absorptivity of 22.7 M^{-1} cm^{-1}. Simultaneously, the change in the concentration of AgNPs can be monitored at wavelengths between 400 and 450 nm, with 415 nm chosen for this study. A Cary 50 UV−visible spectrophotometer operating in kinetic scan mode was employed to monitor the absorbance measurements as a function of time after AgNP addition to the H_2O_2 solution. Scans were acquired over 250−550 nm every 15 s for 5 min.

The concentration of Ag^+ in solution was determined using an Orion 9616BNWP silver/sulfide combination electrode (Thermo-Scientific). The probe was calibrated each day using solutions containing 1, 2, 5, 10, and 20 μM of Ag^+ in pH 9.5 bicarbonate buffer solution.

Analysis of Superoxide Produced from the Reaction between Silver Nanoparticle and H_2O_2. The formation of superoxide from the reaction between AgNPs and H_2O_2 was monitored using the chemiluminescence-based MCLA method.[33,34] A peristaltic pump was used to separately deliver the experimental solution and MCLA reagent into the flow cell of a FeLume CL system (Waterville Analytical) at a flow rate of 3.8 mL min^{-1}. Mixing of the MCLA reagent and sample yielded superoxide-specific CL that was detected by the instrument's photomultiplier tube. The $O_2^{\bullet-}$ concentration in the experimental solution was monitored for 5 min. The system was calibrated in a manner identical to that described by Jones et al.[19] and involved standard addition of photochemically generated superoxide stock into pH 9.5 bicarbonate buffer containing 2.5 μM AgNPs. Subsequently, the FeLume signal corresponding to superoxide concentration at time zero was calculated by extrapolation of the signal to time zero using a log−linear plot. A calibration curve was then constructed from a log−log plot of the photomultiplier tube (PMT) signal versus superoxide concentration.[19]

Detection of Hydroxyl Radicals. The possible formation of hydroxyl radicals was ascertained using a "trip-and-trigger" method whereby any $^{\bullet}OH$ radicals generated react with Phth, producing, among other species, the chemiluminescent 5-hydroxy species.[35] To monitor the production of $^{\bullet}OH$ from the reaction between AgNPs and H_2O_2, 0.55 mM Phth solution was added to the pH 9.5 bicarbonate buffer. Following the addition of AgNPs and H_2O_2, a number of samples were acquired for subsequent analysis using the method described by Miller et al.[36] The effect of the hydroxyl radical scavenger TBA on the ability of AgNPs to degrade H_2O_2 was ascertained by monitoring the rate of H_2O_2 degradation in the presence of 10, 100, and 500 mM TBA.

Kinetic Modeling and Sensitivity Analysis. Speciation calculations were performed using Visual MINTEQ (Version 2.61, KTH Stockholm), while kinetic modeling was undertaken using the software Acuchem.[36] Analysis of the sensitivity of species concentrations in the model to perturbations in various rate constants was undertaken by determining normalized sensitivity coefficients (NSCs) following previously published methods.[37,38] NSCs were determined numerically at 10 equally spaced time intervals over a 10 min duration of the reaction between AgNPs and H_2O_2.

RESULTS AND DISCUSSIONS

Decomposition of H_2O_2. Results of the decay of H_2O_2 following the addition of AgNPs to pH 9.5 bicarbonate buffer containing a known initial concentration of H_2O_2 are shown in Figure 1. Overall, we might expect that the decay of H_2O_2 would be a second-order process with dependencies on the concentrations of both AgNP and H_2O_2; i.e.

$$-\frac{d[H_2O_2]}{dt} = k[AgNP][H_2O_2] \quad (2)$$

where k is a second-order rate constant. Surprisingly, however, particularly in view of the relatively similar initial concentrations of AgNPs and H_2O_2 used in our investigations, peroxide decay follows pseudo-first-order rather than second-order kinetics; i.e.

$$-\frac{d[H_2O_2]}{dt} = k_{obs}[H_2O_2] \quad (3)$$

As shown in the Supporting Information, $\ln\{[H_2O_2]/[H_2O_2]_0\}$ versus time plots are linear in every case with a reasonably

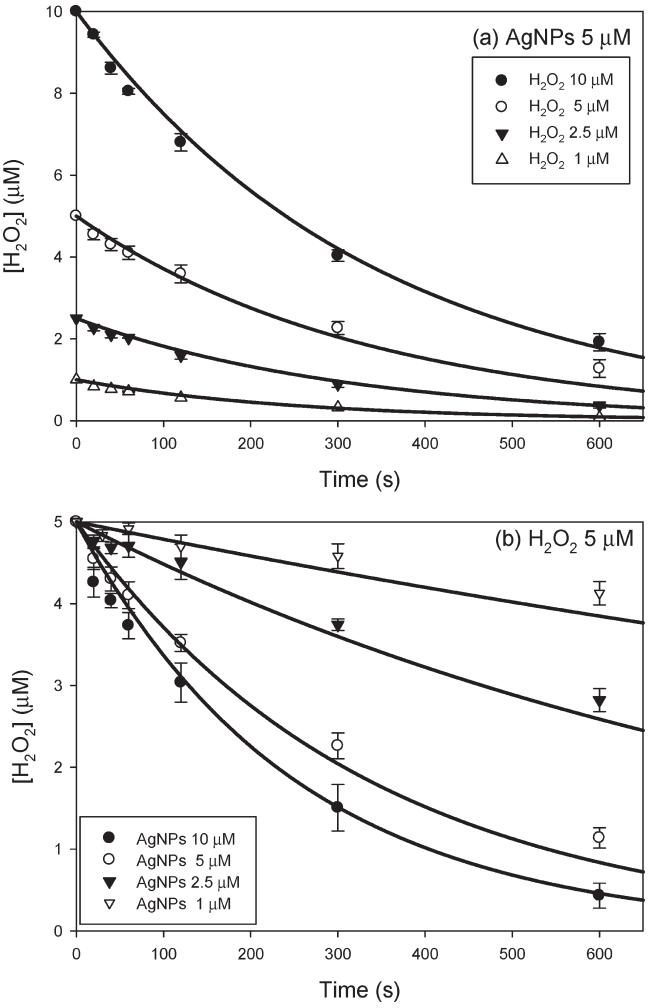

Figure 1. Decomposition of (a) different concentrations of H_2O_2 by 5 μM AgNPs and (b) 5 μM H_2O_2 by different concentrations of AgNPs. Symbols are experimental data; lines are model predictions. Error bars are sample standard deviation from triplicate measurements. AgNPs were prepared via the reduction of 200 μM Ag^+ by photochemically produced superoxide at pH 9.5.

uniform value of k_{obs} ($3.1 \pm 0.7 \times 10^{-3}$ s^{-1}) obtained for the four cases investigated at constant $[AgNP]_0$ and varying $[H_2O_2]_0$. Pseudo-first-order decay of H_2O_2 indicates that the AgNP concentration did not decrease significantly during the process of H_2O_2 degradation and suggests that [AgNP] must be constant throughout the reaction with H_2O_2. The only way in which this can be achieved is for AgNPs to be re-formed as a result of their reaction with peroxide.

According to Guo et al.,[18] the reaction between AgNPs and H_2O_2 involves the formation (in a rate-determining first step) of a reactive intermediate (eq 4) which subsequently reacts rapidly with a second H_2O_2 molecule (eq 5):

$$AgNP + H_2O_2 \xrightarrow{k_2} \text{reactive intermediates (R)} \quad (4)$$

$$\text{reactive intermediates (R)} + H_2O_2 \xrightarrow{k_3} \text{products} \quad (5)$$

Under conditions where $k_2 \ll k_3$, a steady-state concentration of R will be reached and $k_2 = k_{obs}/2[AgNP]$ (see Supporting Information, SI-1). Values of k_2 have been calculated for each

dx.doi.org/10.1021/jp111275a |J. Phys. Chem. C 2011, 115, 5461–5468

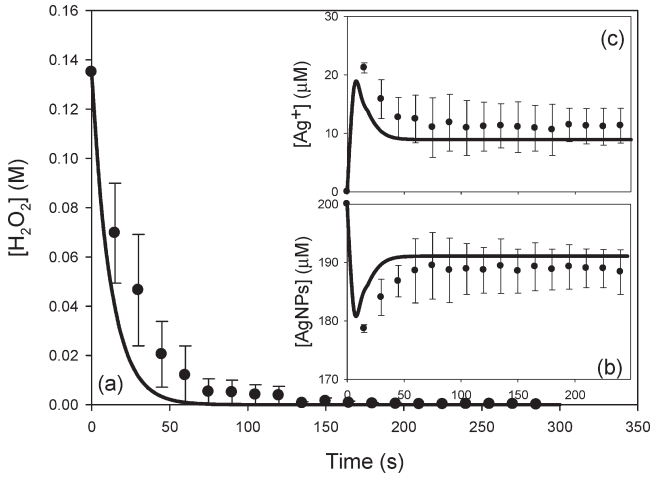

Figure 2. Catalytic decomposition of 135 mM H_2O_2 by 200 μM AgNPs: (a) H_2O_2 decomposition, (b) AgNPs re-formation, and (c) Ag^+ formation. Symbols are experimental data; lines are model predictions. Error bars are sample standard deviations from triplicate measurements. AgNPs were prepared via the reduction of 200 μM Ag^+ by photochemically produced superoxide at pH 9.5.

$[AgNP]_0$ and $[H_2O_2]_0$ pair used with an average ($\pm$SD) value of $2.66 \pm 0.78 \times 10^2$ M^{-1} s^{-1} obtained from the complete data set.

Products of this reaction have been reported to include superoxide.[21,39] Significantly, Guo et al.[18] indicated that when the superoxide scavenger nitro blue tetrazolium and superoxide dismutase were added to the H_2O_2−Ag colloid system, the decomposition of H_2O_2 ceased. The production of superoxide and the apparent re-formation of AgNPs is consistent with the recent confirmation by Jones et al.[19] that superoxide, in the presence of AgNPs, induces reduction of Ag^+ [the dominant Ag(I) species present] with resultant rapid re-formation of AgNPs.

Further evidence for rapid re-formation of AgNPs was provided by catalytic degradation of excess H_2O_2 by AgNPs. As shown in Figure 2a, the addition of excess H_2O_2 (135 mM) to a 200 μM AgNP suspensions is observed to result in the complete consumption of H_2O_2 within 3 min. The data in Figure 2 cannot be explained if the reactions shown in eqs 4 and 5 are the only ones involved, with the obvious need for significant re-formation of AgNPs in order to explain the consumption of such a high concentration of H_2O_2 by the substantially smaller concentration of AgNPs present. As noted above, Jones et al.[19] have confirmed that superoxide is able to reduce Ag^+ to Ag^0 resulting (presumably after the aggregation of the Ag^0 atoms generated in this manner) in the formation of AgNPs though the rate of the homogeneous process (i.e., that occurring in the absence initially of AgNPs):

$$Ag^+ + O_2^{\bullet -} \rightarrow AgNP + O_2 \qquad (6)$$

was found to be slow with a rate constant for this reaction of only 64.5($\pm$16.3) M^{-1} s^{-1}. In comparison, the rate of the reaction was increased by at least 4 orders of magnitude when AgNPs were present. The increase in the rate of reduction of Ag^+ by superoxide in the presence of AgNPs was rationalized by Jones et al[19] using the electron charging and discharging model proposed previously by Henglein.[40] Henglein[40] reported that when organic free radicals were produced in aqueous solutions of silver nanoparticles, the radicals transfer electrons to the silver nanoparticles. These particles acquired a stationary negative charge and thus represent an electron pool from which charge can be extracted singly or pairwise by suitable acceptors in solution. Oxygen, water, and ions such as Ag^+ may act as acceptors. Jones et al.[19] proposed that superoxide, in a manner analogous to ketyl radicals examined by Henglein,[40] may also charge the AgNPs with subsequent transfer of electrons from the charged particles to Ag^+ and oxygen with resultant re-formation of AgNPs:

$$AgNP + O_2^{\bullet -} \rightarrow AgNP^{*-} + O_2 \qquad (7)$$

$$AgNP^{*-} + O_2 \rightarrow AgNP + O_2^{\bullet -} \qquad (8)$$

$$AgNP^{*-} + Ag^+ \rightarrow AgNP + AgNP \qquad (9)$$

where "$AgNP^{*-}$" represents a particle that has received electrons from superoxide. As indicated by Henglein and Lilie,[41] the charging process (eq 7) is diffusion-controlled and takes place within milliseconds. The discharging reactions (eqs 8 and 9) occur at slower rates with the actual rate purported to be dependent on the number of electrons stored. Indeed, Henglein[41,42] represented charged AgNP particles as "Ag_n^{m-}", where m is the charge of elemental silver particles and n is the number of silver atoms, with the "discharge" reaction between the charged nanoparticle and Ag^+ ions written as

$$Ag_n^{m-} + Ag^+ \rightarrow Ag_{n+1}^{(m-1)-} \qquad (10)$$

Given that the diameter of an Ag atom is 0.288 nm, a 5 nm diameter nanoparticle would contain approximately 4000 atoms and a 20 nm diameter particle on the order of 250 000 silver atoms. Different-sized nanoparticles would be expected to exhibit different charge and discharge behavior and, as shown later, this is indeed the case. For simplicity of analysis and to facilitate the kinetic modeling however, we will continue to represent the charged nanoparticles as $AgNP^{*-}$ and determine rate constants for reactions of $AgNP^{*-}$ that are formed from AgNP nanoparticles of a particular size distribution.

Using this simplification, an analogous electron charging−discharging model to that proposed by Jones et al.[19] and incorporating the reaction set shown in Table 1 was employed to account for the interactions among AgNPs, Ag^+, superoxide, and H_2O_2 here. As can be seen from the model fits shown in Figures 1 and 2, this reaction set is able to satisfactorily describe the H_2O_2 degradation data at both low and higher initial concentrations of H_2O_2. The model also provides excellent fits to the time variation in AgNP and Ag^+ concentrations (Figure 2b,c) with initial significant perturbations following mixing of AgNP and H_2O_2 but with AgNP concentration approaching the original concentration after 1−2 min and, on a similar time scale, Ag^+ concentration approaching a steady-state value of ~10 μM.

Formation of Superoxide. The results of measurement of the concentration of superoxide following the addition of AgNPs to the solution containing H_2O_2 using the MCLA method are shown in Figure 3 and indeed confirm that superoxide is formed. The superoxide concentration is observed to rise rapidly in the first few seconds after adding the AgNPs to the H_2O_2 solutions but then approaches steady-state concentrations of 4, 11, and 16 nM in suspensions containing 2.5 μM AgNP and 1, 10, and 20 μM H_2O_2, respectively. As can be seen in Figure 3, application of the electron charging−discharging model described above (and shown in Table 1) provides an excellent description of the superoxide profiles observed in these studies, though the model does predict a slightly more rapid decrease in steady-state superoxide concentration than is observed experimentally.

Table 1. Proposed Model for the Catalytic Decomposition of H_2O_2 by AgNPs in pH 9.5 Bicarbonate Buffer[a]

no.	reaction	k (M^{-1} s^{-1})	comments	reference
1	$O_2^{\bullet -} + O_2^{\bullet -} + 2H^+ \rightarrow H_2O_2 + O_2$	1.9×10^3		16
2	$AgNP + H_2O_2 \rightarrow$ intermediates	$2.66(\pm 0.78) \times 10^2$	dependent on the AgNP size	this study
3	intermediates $+ H_2O_2 \rightarrow Ag^+ + O_2^{\bullet -} + 2H_2O_2$	$>1.0 \times 10^7$	fast	this study
4	$Ag^+ + O_2^{\bullet -} \rightarrow AgNP + O_2$	$64.5(\pm 16.3)$		
5	$AgNP + O_2^{\bullet -} \rightarrow AgNP^{*-} + O_2$	1.0×10^{10}	diffusion-controlled reaction	19,
6	$AgNP^{*-} + O_2^{\bullet -} \rightarrow AgNP + O_2^{\bullet -}$	2.0×10^9	fast	19, 41
7	$AgNP^{*-} + Ag^+ \rightarrow AgNP + AgNP$	7.0×10^8	dependent on the AgNP size	this study
8	$AgNP + O_2 \rightarrow Ag^+ + O_2^{\bullet -}$	<0.01		10

[a] AgNPs were prepared via reduction of 200 μM Ag^+ by photochemically produced superoxide.

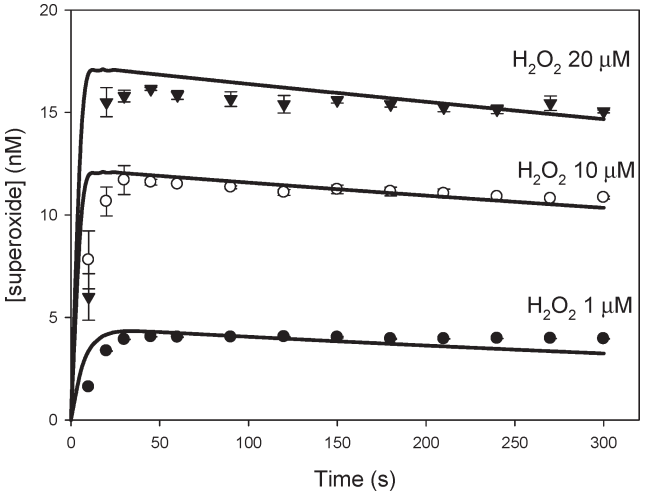

Figure 3. Production of superoxide following the reaction of AgNPs and H_2O_2. Symbols are experimental data; lines are model predictions. Experimental conditions: $[AgNP]_0 = 2.5$ μM. Error bars are sample standard deviations from triplicate measurements. AgNPs were prepared via the reduction of 200 μM Ag^+ by photochemically produced superoxide at pH 9.5.

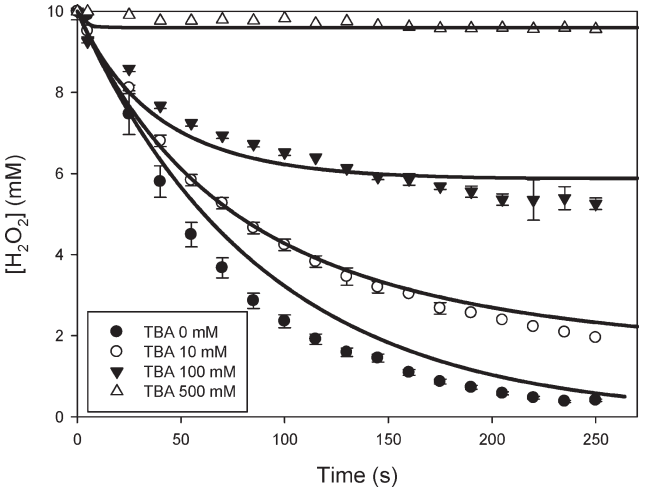

Figure 4. Effect of *tert*-butyl alcohol (TBA) on the catalytic decomposition of H_2O_2 by AgNPs. Symbols are experimental data; lines are model predictions. Experimental conditions: $[AgNP]_0 = 20$ μM, $[H_2O_2]_0 = 10$ mM. Error bars are sample standard deviations from triplicate measurements. AgNPs were prepared via the reduction of 200 μM Ag^+ by photochemically produced superoxide at pH 9.5.

Detection of Strongly Oxidizing Species. The best known means of producing powerful oxidizing species such as the hydroxyl radical is via the Haber–Weiss mechanism[43] typically involving the peroxidation of Fe(II) or Cu(I) species. A similar process involving reaction between Ag^0 and H_2O_2 could be envisaged to occur here; i.e.[18]

$$AgNP + H_2O_2 \rightarrow Ag^+ + {}^{\bullet}OH + OH^- \quad (11)$$

$$^{\bullet}OH + H_2O_2 \rightarrow O_2^{\bullet -} + H_2O + H^+ \quad (12)$$

However, no evidence was found for the generation of $^{\bullet}OH$ using the Phth trap-and-trigger method despite sufficient concentration of Phth (0.55 mM) being used to ensure the scavenging of $^{\bullet}OH$ by 2 mM bicarbonate buffer (with $k = 4.0 \times 10^7$ M^{-1} s^{-1} at pH 9.5) and 10 mM (or less) H_2O_2 (with $k = 3.8 \times 10^7$ M^{-1} s^{-1}) was outcompeted by Phth (with $k = 6.0 \times 10^9$ M^{-1} s^{-1}).[35,44,45]

While we did not detect $^{\bullet}OH$ using the phthalhydrazide trap-and-trigger method, the addition of *tert*-butyl alcohol (TBA), a common $^{\bullet}OH$ scavenger, was observed to result in a decrease in the rate of AgNP-mediated H_2O_2 degradation. Model fitting of the data (Figure 4) suggested that the rate constant of the reaction between the reactive intermediates and TBA is around 3 orders of magnitude less than that with H_2O_2. Assuming that reaction 3 is diffusion controlled, the maximum rate constant of the reaction between intermediates and TBA is around 1.0×10^7 M^{-1} s^{-1}, which is around 2 orders of magnitude less than the second-order rate constant of the reaction between free $^{\bullet}OH$ and TBA (2.0×10^9 M^{-1} s^{-1}).[44] The low value of this rate constant (compared to that expected for the reaction between $^{\bullet}OH$ and TBA) combined with the lack of evidence for the generation of free $^{\bullet}OH$ leads to the conclusion that, while a hydroxylating species is being generated in the reaction between AgNPs and H_2O_2, this strong oxidizing species is unlikely to be free $^{\bullet}OH$ and will be referred to hereafter simply as a "reactive intermediate". The nature of this reactive intermediate is unclear but could be in the form of "bound hydroxyl radicals", as used to describe nonhydroxyl oxidants generated in the Fenton system;[46,47] i.e.

$$AgNP + H_2O_2 \rightarrow Ag - O(H) - OH \quad (13)$$

$$Ag - O(H) - OH + H_2O_2 \rightarrow Ag^+ + O_2^{\bullet -} + 2H_2O \quad (14)$$

dx.doi.org/10.1021/jp111275a |J. Phys. Chem. C 2011, 115, 5461–5468

Table 2. Properties of AgNPs Produced via the Reduction of Different Concentrations of Ag^+ by Photochemically Produced Superoxide

initial Ag^+ concentration (μM)	30	60	100	200
average particle size (nm) (weighed by intensity)	69.4	47.2	29.7	25.0
dominant particle size (>90%) (nm) (weighed by volume)	11.4 ± 3.0	9.0 ± 2.4	5.5 ± 1.7	2.9 ± 2.1
ζ-potential (mV)	−24.8	−28.4	−32.5	−30.6
surface plasmon resonance peak (nm)	432	417	409	406
specific visible absorbance ($M^{-1}c\ m^{-1}$)	8967	11066	10610	9375
reaction between AgNPs and H_2O_2 (k_2, $M^{-1}\ s^{-1}$)	35	95	120	270
reaction between charged AgNPs and Ag^+ ions (k_7, $M^{-1}\ s^{-1}$)	2.0×10^6	8.0×10^7	2.0×10^8	7.0×10^8

Alternatively, Ag(II) species have previously been proposed to form on reaction of Ag(I) with free $^{\bullet}OH$[46] and could be involved here:

$$AgNP + H_2O_2 \rightarrow AgOH^+ + OH^- \quad (15)$$

$$AgOH^+ + H_2O_2 + OH^- \rightarrow Ag^+ + O_2^{\bullet -} + 2H_2O \quad (16)$$

Whatever the nature of the reactive intermediate formed here, the overall stoichiometry of the process as well as the end products produced appear to be in accord with the reactions presented above.

Effect of Nanoparticle Size on H_2O_2 Decomposition. AgNPs with different sizes were synthesized via the reduction of different concentrations of Ag^+ by photochemically produced superoxide. As shown in Table 2, the synthesized AgNPs exhibited different average particle sizes, surface plasmon resonance (SPR) peaks, and dominant particle sizes (relative abundance >90%). As the concentration of Ag^+ increased from 30 to 200 μM, the average size of AgNPs decreased from 65.4 to 25.0 nm. On the basis of speciation calculations using Visual MINTEQ,[48] however, further increase in Ag^+ concentration led to the formation of Ag_2CO_3(s) particles, which accelerated the precipitation of AgNPs and thereby prevented accurate measurement of the size of AgNPs using the Zetasizer. In addition, red shifts in the maximum surface plasmon resonance peak occurred with an increase in the size of AgNPs, in accord with results reported by Choi and Hu.[15] Ten minutes after the mixing of 5 μM H_2O_2 and 5 μM AgNPs, the residual concentrations of H_2O_2 were 1.2, 2.9, 3.1, and 4.3 μM when AgNPs were prepared using Ag^+ concentrations of 200, 100, 60, and 30 μM, respectively, indicating that more extensive decomposition of H_2O_2 occurred in the presence of AgNPs of smaller size, as shown in Figure 5a. At the low H_2O_2 concentrations used in these particular studies, reaction 2 is the only important reaction in the model according to sensitivity analysis (Supporting Information, SI-2) and, as such, its rate constant can be determined from the H_2O_2 decay kinetics data. Results are summarized in Table 2 and plotted in Figure 6a. The values of k_2 correlate linearly with the average particle sizes (R^2 = 0.884) and dominant particle sizes (relative abundance >90%) (R^2 = 0.921), showing clearly that the reactivity of AgNPs increases with decreasing size.

In terms of the AgNP-catalyzed decomposition of high concentrations of H_2O_2 (Figure 5b), both reaction 2 and the electron charging−discharging reaction set, especially reaction 7, play significant roles in the degradation of H_2O_2, as shown in Supporting Information, SI-2. As indicated by Henglein and

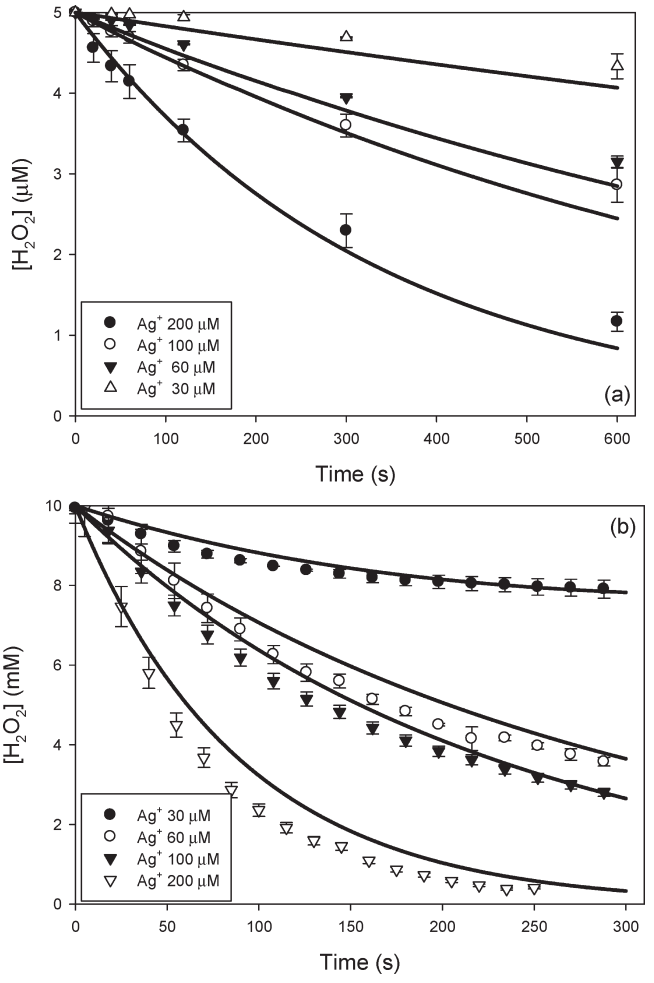

Figure 5. Decomposition of H_2O_2 by AgNPs produced via the reduction of different concentrations of Ag^+ by photochemically produced superoxide. Symbols are experimental data; lines are model predictions. Experimental conditions: (a) $[AgNP]_0$ = 5 μM, $[H_2O_2]_0$ = 5 μM; (b) $[AgNP]_0$ = 20 μM, $[H_2O_2]_0$ = 10 mM. Error bars are sample standard deviations from triplicate measurements.

Lilie,[41] the rate of the discharge reaction depends on the number of electrons stored on each silver particle. AgNPs with smaller sizes are presumably able to store a larger number of electrons for the same mass of silver, thereby accelerating electron transfer to an electron acceptor. Using the k_2 values determined above for particles of different size, the rate constants of reaction 7 (k_7) can

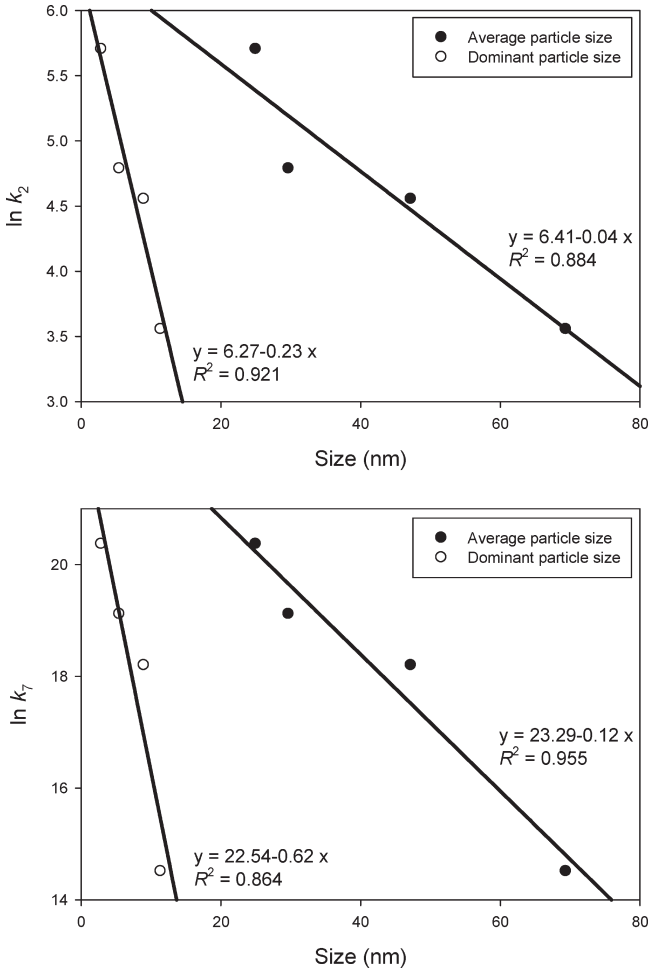

Figure 6. Correlation between second-order rate constants of reaction between particle size with (a) the reaction between AgNPs and H_2O_2 (reaction 2) and (b) the reaction between charged AgNPs and Ag^+ (reaction 7).

be deduced and are shown in Table 2. The correlation between the sizes of AgNPs and k_7 ($R^2 > 0.864$) in Figure 6b further demonstrates that AgNPs of smaller sizes are beneficial to the transfer of electrons from charged AgNPs to Ag^+ with resultant re-formation of AgNPs.

Remaining Uncertainties. The reaction scheme shown in Figure 7 summarizes the most important features of the proposed model for the interactions among AgNPs, H_2O_2, and superoxide. However, significant uncertainties with regard to aspects of the behavior of AgNPs in oxygenated solutions remain, including (1) the rate and extent of oxidation of AgNPs by oxygen and (2) the nature and fate of reactive intermediates.

Liu and Hurt[10] observed the slow generation of H_2O_2 following the oxidation of AgNPs in air-saturated aqueous solutions and suggested that $O_2^{\bullet-}$, a precursor of H_2O_2, was most likely formed via the oxidation of AgNPs by oxygen; i.e.,

$$\text{AgNP} + O_2 \rightarrow Ag^+ + O_2^{\bullet-} \qquad (17)$$

According to Liu and Hurt,[10] the second-order rate constant of the reaction shown in eq 17 was ~0.014 M^{-1} s^{-1} under neutral conditions. The Ag^+ release rate decreased with increasing pH, suggesting that the rate constant would be much less than 0.01 M^{-1} s^{-1} at pH 9.5. In addition, no evidence was found for the

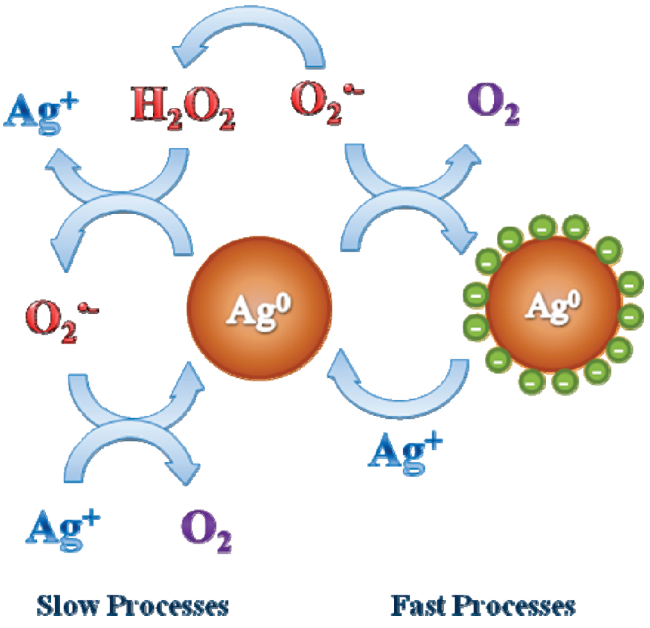

Figure 7. Schematic presentation of the action of AgNPs as electron pool in ROS reactions.

generation of Ag^+ within several hours using a silver/sulfide combination electrode at pH 9.5. Due to the low value of this rate constant (<0.01 M^{-1} s^{-1}), this reaction is expected to have no influence on AgNP-mediated degradation of H_2O_2 but could be an important initiator of the re-formation of AgNPs in solutions in which H_2O_2 is initially absent.

"Bound hydroxyl radicals" or some form of Ag(II) species have been proposed as reactive intermediates in this study. Due to the absence of any available method for detection of the reactive intermediate, it is impossible to determine the rate constant of reaction between this species and H_2O_2 (reaction 3), though, as noted earlier, it is expected to be rapid, at least in comparison to its rate of production via reaction 2. Much remains unknown, however, with regard to the nature and reactivity of this intermediate with these matters likely to be the subject of ongoing investigations by both ourselves and others.

CONCLUSIONS

We have demonstrated here that AgNPs are able to catalyze the decomposition of H_2O_2 in bicarbonate buffer at pH 9.5 with this process attributed to the rapid re-formation of AgNPs resulting from the reaction between Ag^+ and superoxide in the presence of AgNPs. The re-formation of AgNPs facilitates the redox cycling of silver under alkaline conditions, extending the lifetime of AgNPs and allowing them to be employed in catalytic quantities. An electron charging−discharging model was found to successfully describe the interaction of H_2O_2 with AgNPs. The second-order rate constants for the reaction between AgNPs and H_2O_2 ranged from 35 to 2.7 × 10^2 M^{-1} s^{-1} for AgNP particle sizes from 25.0 to 69.4 nm, respectively. A powerful oxidant was produced in the reaction of AgNPs with H_2O_2, but various lines of evidence confirmed that the oxidizing species was not the free hydroxyl radical. This oxidizing species may well be central to the bactericidal properties of AgNPs, but further investigations into the nature and reactivity of this species are required.

dx.doi.org/10.1021/jp111275a |J. Phys. Chem. C 2011, 115, 5461–5468

■ ASSOCIATED CONTENT

Supporting Information. Two figures and one table show additional details of rate constant calculation and sensitivity analysis. This material is available free of charge via the Internet at http://pubs.acs.org.

■ AUTHOR INFORMATION

Corresponding Author
*E-mail: d.waite@unsw.edu.au.

■ ACKNOWLEDGMENT

Assistance provided in use of the phthalhydrazide trap-and-trigger method for hydroxyl radical quantification by Christopher Miller is gratefully acknowledged.

■ REFERENCES

(1) Nel, A.; Xia, T.; Madler, L.; Li, N. *Science* **2006**, *311*, 622.
(2) Pal, S.; Tak, Y. K.; Song, J. M. *Appl. Environ. Microb.* **2007**, *73*, 1712.
(3) Morones, J. R.; Elechiguerra, J. L.; Camacho, A.; Holt, K.; Kouri, J. B.; Ramirez, J. T.; Yacaman, M. J. *Nanotechnology* **2005**, *16*, 2346.
(4) Hwang, E. T.; Lee, J. H.; Chae, Y. J.; Kim, Y. S.; Kim, B. C.; Sang, B. I.; Gu, M. B. *Small* **2008**, *4*, 746.
(5) Smetana, A. B.; Klabunde, K. J.; Marchin, G. R.; Sorensen, C. M. *Langmuir* **2008**, *24*, 7457.
(6) Kohn, T.; Nelson, K. L. *Environ. Sci. Technol.* **2007**, *41*, 192.
(7) Kim, J. S.; Kuk, E.; Yu, K. N.; Kim, J.-H.; Park, S. J.; Lee, H. J.; Kim, S. H.; Park, Y. K.; Park, Y. H.; Hwang, C.-Y.; Kim, Y.-K.; Lee, Y.-S.; Jeong, D. H.; Cho, M.-H. *Nanomed. Nanotechnol.* **2007**, *3*, 95.
(8) Foldbjerg, R.; Olesen, P.; Hougaard, M.; Dang, D. A.; Hoffmann, H. J.; Autrup, H. *Toxicol. Lett.* **2009**, *190*, 156.
(9) Su, H. L.; Chou, C. C.; Hung, D. J.; Lin, S. H.; Pao, I. C.; Lin, J. H.; Huang, F. L.; Dong, R. X.; Lin, J. J. *Biomaterials* **2009**, *30*, 5979.
(10) Liu, J. Y.; Hurt, R. H. *Environ. Sci. Technol.* **2010**, *44*, 2169.
(11) Mendis, E.; Rajapakse, N.; Byun, H. G.; Kim, S. K. *Life Sci.* **2005**, *77*, 2166.
(12) Pal, S.; Tak, Y. K.; Joardar, J.; Kim, W.; Lee, J. E.; Han, M. S.; Song, J. M. In *International Conference on Bionano Science (ICONBS 2007)* Taipei, Taiwan, 2007; Vol. 9, p 2092.
(13) Inoue, Y.; Hoshino, M.; Takahashi, H.; Noguchi, T.; Murata, T.; Kanzaki, Y.; Hamashima, H.; Sasatsu, M. *J. Inorg. Biochem.* **2002**, *92*, 37.
(14) Chang, Q. Y.; Yan, L. Z.; Chen, M. X.; He, H.; Qu, J. H. *Langmuir* **2007**, *23*, 11197.
(15) Choi, O.; Hu, Z. Q. *Environ. Sci. Technol.* **2008**, *42*, 4583.
(16) Bielski, B. H. J.; Cabelli, D. E.; Arudi, R. L.; Ross, A. B. *J. Phys. Chem. Ref. Data* **1985**, *14*, 1041.
(17) Endo, T.; Yanagida, Y.; Hatsuzawa, T. *Measurement* **2008**, *41*, 1045.
(18) Guo, J. Z.; Cui, H.; Zhou, W.; Wang, W. *J. Photochem. Photobiol. A* **2008**, *193*, 89.
(19) Jones, A. M.; Garg, S.; He, D.; Pham, A. N.; Waite, T. D. *Environ. Sci. Technol.* **2011**, *45*, 1428.
(20) El Badawy, A. M.; Luxton, T. P.; Silva, R. G.; Scheckel, K. G.; Suidan, M. T.; Tolaymat, T. M. *Environ. Sci. Technol.* **2010**, *44*, 1260.
(21) Tan, S.; Erol, M.; Attygalle, A.; Du, H.; Sukhishvili, S. *Langmuir* **2007**, *23*, 9836.
(22) Morgan, M. S.; Vantrieste, P. F.; Garlick, S. M.; Mahon, M. J.; Smith, A. L. *Anal. Chim. Acta* **1988**, *215*, 325.
(23) Garg, S.; Rose, A. L.; Waite, T. D. *Photochem. Photobiol.* **2007**, *83*, 904.
(24) Jose, T. P.; Tuwar, S. M. *J. Mol. Struct.* **2007**, *827*, 137.
(25) Huang, H. H.; Ni, X. P.; Loy, G. L.; Chew, C. H.; Tan, K. L.; Loh, F. C.; Deng, J. F.; Xu, G. Q. *Langmuir* **1996**, *12*, 909.
(26) Ji, M.; Chen, X. Y.; Wai, C. M.; Fulton, J. L. *J. Am. Chem. Soc.* **1999**, *121*, 2631.
(27) Kapoor, S. *Langmuir* **1998**, *14*, 1021.
(28) Mock, J. J.; Barbic, M.; Smith, D. R.; Schultz, D. A.; Schultz, S. *J. Chem. Phys.* **2002**, *116*, 6755.
(29) Finsy, R. *Adv. Colloid Interface Sci.* **1994**, *52*, 79.
(30) Koppel, D. E. *J. Chem. Phys.* **1972**, *57*, 4814.
(31) Towne, V.; Will, M.; Oswald, B.; Zhao, Q. J. *Anal. Biochem.* **2004**, *334*, 290.
(32) Zhou, M. J.; Diwu, Z. J.; PanchukVoloshina, N.; Haugland, R. P. *Anal. Biochem.* **1997**, *253*, 162.
(33) Nishida, A.; Kimura, H.; Nakano, M.; Goto, T. *Clin. Chim. A.* **1989**, *179*, 177.
(34) Rose, A. L.; Waite, T. D. *Environ. Sci. Technol.* **2005**, *39*, 2645.
(35) Miller, C.; Rose, A.; Waite, T. D. *Anal. Chem.* **2011**, *83*, 261.
(36) Braun, W.; Herron, J. T.; Kahaner, D. K. *Int. J. Chem. Kinet.* **1988**, *20*, 51.
(37) Rose, A. L.; Waite, T. D. *Aquat. Sci.* **2003**, *65*, 375.
(38) Pham, A. N.; Waite, T. D. *Geochim. Cosmochim. Acta* **2008**, *72*, 3616.
(39) Ono, Y.; Matsumura, T.; Kitajima, N.; Fukurumi, S.-I. *J. Phys. Chem.* **1977**, *81*, 1307.
(40) Henglein, A. *J. Phys. Chem.* **1979**, *83*, 2209.
(41) Henglein, A.; Lilie, J. *J. Am. Chem. Soc.* **1981**, *103*, 1059.
(42) Henglein, A. *Langmuir* **2001**, *17*, 2329.
(43) Haber, F.; Weiss, J. *Proc. R. Soc. A.* **1934**, *147*, 332.
(44) Buxton, G. V.; Greenstock, C. L.; Helman, W. P.; Ross, A. B. *J. Phys. Chem. Ref. Data* **1988**, *17*, 513.
(45) Alegre, M. L.; Gerones, M.; Rosso, J. A.; Bertolotti, S. G.; Braun, A. M.; Martire, D. O.; Gonzalez, M. C. *J. Phys. Chem. A* **2000**, *104*, 3117.
(46) Rush, J. D.; Koppenol, W. H. *J. Inorg. Biochem.* **1987**, *29*, 199.
(47) Sawyer, D. T.; Kang, C.; Llobet, A.; Redman, C. *J. Am. Chem. Soc.* **1993**, *115*, 5817.
(48) Gustafsson, J. P. *Visual MINTEQ*; Department of Land and Water Resources Engineering, KTH: Stockholm, Sweden, 2009.